



Title	Generation of ultrashort optical pulses in the 10 fs regime using multicolor Raman sidebands in KTaO ₃
Author(s)	Matsubara, Eiichi; Kawamoto, Yuta; Sekikawa, Taro; Yamashita, Mikio
Citation	Optics Letters, 34(12), 1837-1839 https://doi.org/10.1364/OL.34.001837
Issue Date	2009-06-15
Doc URL	http://hdl.handle.net/2115/45305
Rights	© 2009 Optical Society of America
Type	article
File Information	OL34-12_1837-1839.pdf



[Instructions for use](#)

Generation of ultrashort optical pulses in the 10 fs regime using multicolor Raman sidebands in KTaO_3

Eiichi Matsubara,* Yuta Kawamoto, Taro Sekikawa, and Mikio Yamashita

Department of Applied Physics, Graduate School of Engineering, Hokkaido University, and CREST, Japan Science and Technology Agency Kita-13, Nishi-8, Kita-ku, Sapporo, 060-8628, Japan

*Corresponding author: matsu-e@eng.hokudai.ac.jp

Received January 13, 2009; revised April 21, 2009; accepted May 6, 2009;
posted May 14, 2009 (Doc. ID 106163); published June 9, 2009

We demonstrated Fourier synthesis of a new type of multiple coherent anti-Stokes Raman scatterings in KTaO_3 crystal. The signals with a wavelength range of 500–750 nm were generated by two femtosecond pulses whose frequency difference was set to be a two-phonon Raman frequency. Angle dispersion of the signals was compensated into one white-continuum beam by spherical mirrors and a prism. The spectral phase, measured by spectral phase interferometry for direct electric-field reconstruction, was compensated for by carefully aligning the angle and the position of the optical components so that 13 fs isolated pulses were generated. This result shows the robustness of our scheme to produce ultrashort optical pulses.

© 2009 Optical Society of America

OCIS codes: 190.4720, 300.6230, 320.5520, 320.5540.

Generation of multiple coherent anti-Stokes Raman scattering (CARS) in crystals under pumping by two color femtosecond laser pulses has been intensively studied by several groups [1–3], especially for the production of extremely short optical pulses, while the generation of a train of 1.6 fs pulses using Raman sidebands of D_2 gas was reported in 2005 [4]. Advantages of crystals over gases as Raman media to produce extremely short pulses are 1) an isolated pulse can be generated owing to the continuous entire intensity spectrum and 2) the spectral phase can be characterized by some methods such as spectral phase interferometry for direct electric-field reconstruction (SPIDER) [5], so that prompt and appropriate temporal dispersion compensation is possible by using a programmable liquid-crystal spatial light modulator [6]. The only disadvantage was that the signals have large angle dispersion, because two pumping beams are forced to be noncollinear, which had been a crucial matter.

Recently, we have overcome the problem and succeeded in generating an isolated 25 fs pulse using the “conventional” multiple CARS signals in a single crystal of LiNbO_3 , where both the angle dispersion and the temporal dispersion compensation were achieved by a configuration with one spherical mirror and a grating [7]. In the present Letter, we report the drastic shortening of the pulse duration down to 13 fs, which has been achieved by the use of a new type of multiple CARS signal, called Raman–Nathlike (RN) CARS, from KTaO_3 crystal. RN-CARS has two advantages over the conventional CARS for the generation of ultrashort pulses. It is empirically known and theoretically supported that RN-CARS can generate higher-order CARS signals than the conventional process [8]. Because of this, the spectral width covered by RN-CARS is expected to be broader than that by the conventional one and, consequently, the Fourier transform-limited pulse duration be-

comes shorter. Figure 1 shows the schematics of the angle dispersions of (a) the conventional CARS and (b) the RN-CARS. The angle distribution of RN-CARS has an almost linear relationship, while that of the conventional CARS has nonlinear one. Hence, this angle dispersion of RN-CARS can be compensated for using a prism with higher diffraction efficiency than a grating [9]. Therefore RN-CARS enables us to generate more intense ultrashort pulses. This different angle dispersion of RN-CARS comes from the two-phonon Raman excitation by two optical pulses with wavevectors of \mathbf{k}_1 and \mathbf{k}_2 and, therefore, RN-CARS has different momentum conservation, $\mathbf{k}_{sl} = \mathbf{k}_1 + l(\mathbf{k}_1 - \mathbf{k}_2)_x/2$, from the conventional CARS, $\mathbf{k}_{sl} = \mathbf{k}_1 + l(\mathbf{k}_1 - \mathbf{k}_2)$. Although we do not have enough room to explain why the generated coherent phonons have the momentum of $(\mathbf{k}_1 - \mathbf{k}_2)_x/2$, we would like to point out that the symmetry breaking by the coherent excitation by the laser light excites the Raman mode with $(\mathbf{k}_1 - \mathbf{k}_2)_x/2$. For more detail, please refer to [8,10].

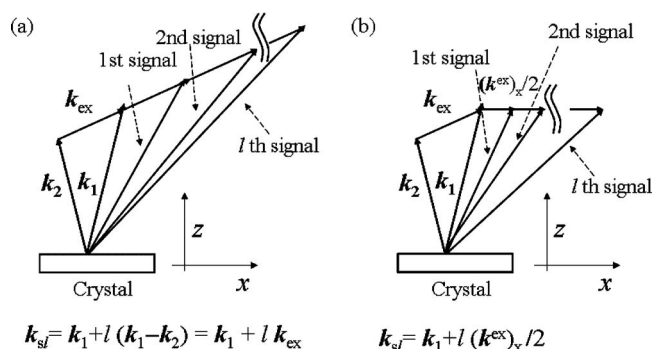


Fig. 1. Illustration to show how angle distributions of (a) the conventional CARS and (b) the RN-CARS differ from each other. Here, \mathbf{k}_1 and \mathbf{k}_2 are wavevectors of incident pulses. \mathbf{k}_{ex} is defined as $\mathbf{k}_1 - \mathbf{k}_2$. \mathbf{k}_{sl} is the wavevector of the l th CARS signal.

The experimental setup is shown in Fig. 2. The signal (ω_1) and idler (ω_2) pulses from an optical parametric amplifier (OPA) pumped by a 30 fs Ti:sapphire laser amplification system were focused by a lens (L) and were simultaneously irradiated onto the (001) surface of a KTAO_3 crystal with a 0.2 mm thickness (KT). The frequency difference of the input pulses was set to be 1130 cm^{-1} in order to resonantly pump a broad two-phonon Raman peak of 2TO_4 mode around 1100 cm^{-1} [11] or other peaks with frequencies less than 1100 cm^{-1} . The ω_1 (ω_2) pulse had a center wavelength of 1476 (1772) nm and a pulse energy of 15 (11) μJ , which was tuned by two variable neutral density filters (VNDs). The duration and the bandwidth of the input pulses were 200–300 fs and a few hundred cm^{-1} , respectively. The crossing angle between the input beams was 8.1 deg in the air and 3.8 deg in the crystal. The polarization of the input pulses was chosen to be vertical and parallel to one of the crystalline axis of KTAO_3 . The multiple CARS signals were generated behind the crystal with finite angle dispersion. The CARS signals were reflected back by a spherical mirror with a focal length of 100 mm (SM1) and were focused onto the surface of an equilateral-triangle prism made of SF18 glass (P). The beam reflected by SM1 was off the plane made by wavevectors of two incident beams and propagated slightly below KT. Accordingly P was also tilted so that normal incidence was achieved vertically. The spot size of the focused beam was approximately 1 mm in diameter. To tune the magnification factor of M , defined as the ratio of the distance between the crystal and the spherical mirror (f_1), and that between the spherical mirror and the prism (f_2) arbitrarily, only one spherical mirror was used. The M value was carefully chosen so that all the signals were diffracted into the same direction; it was 0.14 under the present experimental condition. The diffracted beam was collimated by a spherical mirror with a 500 mm focal length (SM2). In the SPIDER measurement [7], the relative time delay of two replicas was 667 fs, the spectral shear was 3.18 THz (106 cm^{-1}), and the spectral shift given by the chirped reference pulse (divided output from the amplifier) was 366 THz.

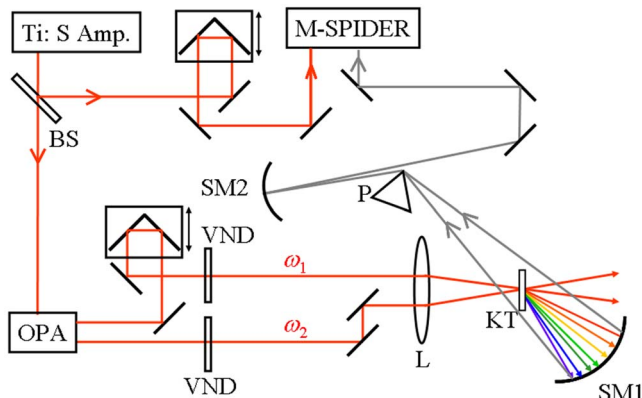


Fig. 2. (Color online) Experimental setup for ultrashort pulse generation using multiple RN-CARS signals.

Figure 3 shows the intensity spectrum and the spectral phase of the angle-dispersion compensated CARS beam. By carefully adjusting the rotation angle and the position of the prism, the spectral phase became almost flat in the frequency range from 15000 to 18000 cm^{-1} within π rad variation, although it increases to 10 rad at approximately 18500 cm^{-1} . The temporal intensity profile of the generated pulse and that of the transform-limited (TL) one are shown in Fig. 4. As is expected from the entire continuous spectrum, an isolated pulse was generated. The duration of the observed pulse is 13 fs, while that of the TL one is 9.8 fs. The use of RN-CARS signals with higher intensity and broader bandwidth has enabled us to generate pulses with shorter duration than that in our previous study [7]. The solid gray curve shows the temporal phase profile, which is almost flat during the pulse duration. The energy of the compressed pulse is estimated to be a several hundred nanojoules.

Now let us discuss the present results. First, we examine the intensity spectrum in more detail. As eye-guided by dashed-dotted vertical lines, the intensity spectrum has peaks with a dominant frequency spacing of 692 cm^{-1} , which is assigned to be $\text{TO}_4 + \text{TO}_1$ mode at the Brillouin zone boundary [11], although the input pulses resonantly pumped 1130 cm^{-1} . We can explain this by considering the dual excitation of Raman peaks at 692 and 465 cm^{-1} , the sum of which is 1157 cm^{-1} . The Raman peak at 465 cm^{-1} is assigned to be $\text{TO}_4 - \text{TA}$ mode [11]. Note that the incident pulses have a bandwidth of 200–300 cm^{-1} . Although multiple peaks with the separation of 465 cm^{-1} are not clearly seen in the spectrum, they are thought to be superimposed in the entire spectrum and be broadening the structure. The discrepancy between the frequency difference of two input pulses and the frequency separation of the generated CARS field is also seen in diamond crystal [2]. There the dependence of the frequency separation of CARS peaks on the relative angle between two incident pulses has been pointed out. Hence such discrepancy is often in the case of crystals.

Second, we consider how the temporal-dispersion compensation of the multiple RN-CARS signals is achieved in the experimental setup. Similarly to the

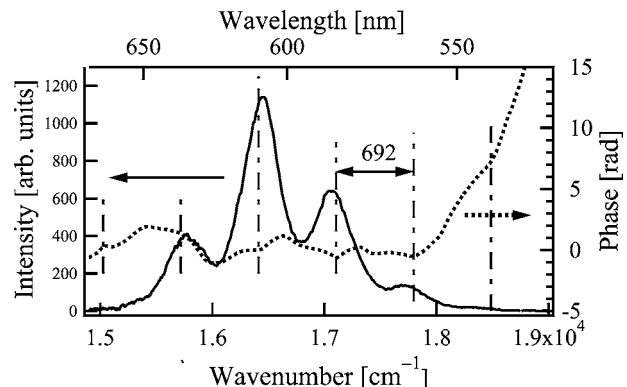


Fig. 3. Intensity spectrum (solid curve) and spectral phase (dotted curve) of the angle-dispersion-compensated multiple RN-CARS signals.

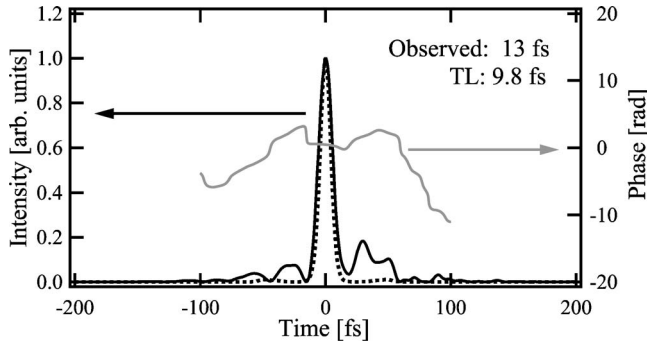


Fig. 4. Temporal intensity profile of a compressed pulse (solid curve) and that of a transform-limited one (dotted curve). The solid gray curve shows temporal phase profile of the compressed pulse.

case of the conventional CARS in LiNbO_3 , the configuration consisting of spherical mirrors and a prism plays the important role [12]. The second-order dispersion (group delay dispersion; GDD) applied by the configuration is given by [7]

$$\frac{d^2\Psi}{d\Omega^2} = -\frac{1}{c}(z'M^2 + z) \left\{ \left(2\frac{da}{d\Omega} + \Omega\frac{d^2a}{d\Omega^2} \right) \sin a + \Omega \left(\frac{da}{d\Omega} \right)^2 \cos a \right\}. \quad (1)$$

Here, a is the diffracted angle of a ray with an angular frequency Ω and is measured with respect to the ray with the center frequency. z is the distance between the crystal and the focal point, and z' is the distance between the focal point and the prism (see Fig. 1(a) in [7]). z (z') is positive if the distance between KT (P) and SM1 is longer than f_1 (f_2) [12]. Note that the paraxial approximation is not used here, because angle dispersion of the signals is so large. Now that we use a prism, instead of a grating, positive-material dispersion given by the SF18 glass must be taken into account. However, a calculation reveals that such positive dispersion can be compensated for as follows. Assume that the 600 nm component propagates through the optical axis of the optical configuration. Using parameters of $z=149.5\ \mu\text{m}$, $z'=1500\ \mu\text{m}$, and $M=0.14$, the total GDD of $355\ \text{fs}^2$ is completely canceled at the center frequency of 600 nm. Here we have assumed that the z is the propagation distance of the RN-CARS signals from the point where two input pulses are overlapped to the rear surface of the crystal, and the angle dispersion of the signals in the crystal as well as that in the

prism are neglected. In the calculation, the total GDD is more sensitive to z than to z' , because M is too small in the present experimental condition.

Finally, we discuss the reason why precision of the temporal dispersion compensation has been improved compared with that in our previous study, where a 25 fs pulse was generated while the duration of the TL one was 11 fs. We think this is because we paid much attention to the angle of the spherical mirror (SM1) in our experimental setup. A tilted spherical mirror with a point source displaced laterally from the center of curvature produces third-order (coma) aberration, which is considered to cause the third-order dispersion (TOD) in dealing with ultrashort pulses [13]. Actually, when the SM1 was laterally tilted, we observed a significant TOD (in the order of several thousand fs^3) left in the spectral phase even if other parameters were well optimized.

In conclusion, we generated an isolated 13 fs optical pulse using a new type of multiple CARS signals from a single crystal of KTaO_3 . The crystal was non-collinearly pumped by two color femtosecond pulses. The angle and the temporal dispersion of the signals were compensated for by a configuration with spherical mirrors and a prism.

References

1. H. Matsuki, K. Inoue, and E. Hanamura, *Phys. Rev. B* **75**, 024102 (2007).
2. M. Zhi, X. Wang, and A. V. Sokolov, *Opt. Express* **16**, 12139 (2008).
3. J. Liu, J. Zhang, and T. Kobayashi, *Opt. Lett.* **33**, 1494 (2008).
4. M. Y. Shverdin, D. R. Walker, D. D. Yavuz, G. Y. Yin, and S. E. Harris, *Phys. Rev. Lett.* **94**, 033904 (2005).
5. M. E. Anderson, L. E. E. de Araujo, E. M. Kosik, and I. A. Walmsley, *Appl. Phys. B* **70**, S85 (2000).
6. A. M. Weiner, D. E. Leaird, J. S. Patel, and J. R. Wullert, *IEEE J. Quantum Electron.* **28**, 908 (1992).
7. E. Matsubara, T. Sekikawa, and M. Yamashita, *Appl. Phys. Lett.* **92**, 071104 (2008).
8. K. Inoue, J. Kato, E. Hanamura, H. Matsuki, and E. Matsubara, *Phys. Rev. B* **76**, 041101 (2007).
9. L. Xu, N. Nakagawa, R. Morita, H. Shigekawa, and M. Yamashita, *IEEE J. Quantum Electron.* **36**, 893 (2000).
10. E. Matsubara, K. Inoue, and E. Hanamura, *Phys. Rev. B* **72**, 134101 (2005).
11. W. G. Nilsen and J. G. Skinner, *J. Chem. Phys.* **47**, 1413 (1967).
12. O. E. Martinez, *IEEE J. Quantum Electron.* **23**, 59 (1987).
13. H. Nishioka, in *Proceedings of 20th Annual Meeting of the IEEE Laser and Electro-Optics Society* (IEEE, 2007) p. 366.